

Spectroscopy of Individual Light-Harvesting Complexes

Martin Clausen

30.5.2002

Abstract

This text gives a short introduction to the spectroscopy of individual light-harvesting complexes. Spectroscopy is a technique with which it is possible to gain information over the transfer of light into an electrochemical potential by photosynthetic organisms. A general introduction is followed by a discussion of a recent article on the light-harvesting complex 2 of *Rhodopseudomonas Acidophila*, a purple bacterium [1].

1 Photosynthesis

The first life on earth probably gained its energy from the breaking down of organic molecules produced by geochemical processes. But soon a much more efficient method for the production of energy was developed. Photosynthetic bacteria started to use light to establish an electrochemical potential across a membrane. This stored energy can be used to convert ADP into ATP, the fuel for nearly all processes in living cells.

All photosynthetic organisms contain light-harvesting antenna systems to utilize solar light. The electromagnetic radiation creates an excitation of the pigments of the antenna system. The excitation is quickly forwarded into the reaction center (RC). There a charge separation takes place, building up an electrochemical potential. This form of energy is far much more stable than the excitation of a pigment, which can not be coupled so efficiently to other rather slow endothermic biochemical processes. The time scale of energy transfer is ranging from fs to ps, for the electron transfer ps, while the ATP synthase processes only some 100 molecules per second [2].

Classification of Photosynthetic Organisms One major difference between photosynthetic organisms is, whether they produce oxygen during the process or not. Plants, algae and cyanobacteria do, while green bacteria, heliobacteria and purple bacteria execute an anoxygenic photosynthesis.

The following text will concentrate on the purple bacteria *Rhodopseudomonas Acidophila* (*Rsp. A.*). Details on the biochemistry of plants and cyanobacteria can be

found in [2], while excitons in the corresponding light-harvesting complexes are described in [3].

1.1 The Photosynthetic Unit of *Rhodopseudomonas Acidophila*

The photosynthetic unit (PSU) of *Rsp. A.* contains a system of light-harvesting complexes (LH1, LH2) and a RC. The RC is build up from a primary chlorophyll, bacteriochlorophyll (BChls), bacteriopheophyrin, ubiquinone-10, magnesium atoms and an iron ion. The light-harvesting system consists of a core antenna, LH1, which for BChl a containing species absorbs around 870 to 880 nm. The BChl of the LH1 form a circle around the RC. LH2 complexes surround the LH1 in the plane of the membrane.

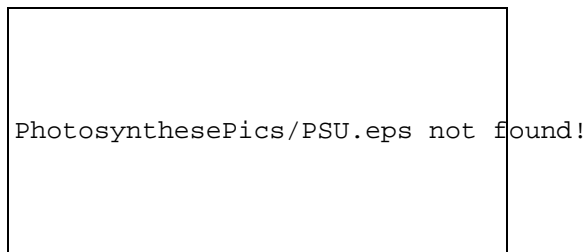


Figure 1: Model of the PSU of purple bacteria based on known structural data, the highlighted ring corresponds to a diameter of about 23 nm, the time constances apply for a temperature of 77 K, Fig. taken from [4].

Structure and Properties of LH2 Recently the three dimensional structure of the LH2 complex was determined through x-ray crystallography. It consists of a ring with in crystalline form nine fold symmetry. LH2 is made up from nine α - β polypeptides heterodimers, which in total bind 27 BChl a molecules and 18 carotenoids. The LH2 can be grouped into two parts: On the cytoplasmic side 9 BChl absorb around 800 nm (B800). They are about 2.1 nm a part and can be therefor described as monomeric. Energy is transfered at a sub ps range. The second part is on the periplasmic side, 1.7 nm away from the other ring. It contains 18 BChls which absorb around 860 nm (B850). The energy can be transfered in this ring within less than 100 fs. These molecules are strongly coupled, because their center-center distance is about 0.9 nm. Excitation energy is

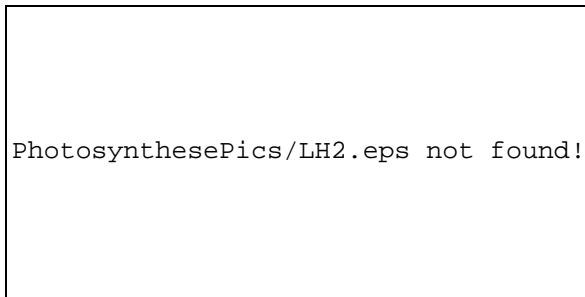


Figure 2: Geometrical arrangement of the 27 BChl molecules of the LH2 complex as determined by x-ray crystallography, the phytol chains are omitted for clarity, Fig. taken from [8].

transfered from the B800 to the B850 ring in about 1 ps with a yield of more than 95%. The carotenoids are bound to the α and β proteins, span the membrane and contact both B800 and B850 BChls.

The carotenoids in photosynthetic pigment protein complexes have in general two major functions: First they quench the triplet states of the BChls. These triplet states not only block the BChl, but may be also transfered to oxygen. The ground state of oxygen is a triplet state, which will be converted to a highly reactive singlet state, if the energy of a BChl in triplet state is transfered to it. The second function is light-harvesting. Excitation energy of the carotenoids is transfered to the B800 and B850 pigments and follows than the way to the RC [4].

2 Molecule Interactions

Molecular interactions are essential for the function of the PSU. They are governed by coulombic interactions of electrons and nuclei of different pigments and the exchange interactions between overlapping molecular orbitals of pigments. In the later case electrons are exchanged between donor (D) and acceptor (A). In general the energy V involved can be described as follows:

$$V_{DA} = \frac{1}{4\pi\epsilon_0} \sum_{i \in D, j \in A} \frac{q_i q_j}{r_{ij}}$$

with ϵ_0 the vacuum permittivity and r_{ij} the distance between the electronic and nuclear charges q_i and q_j on the molecules A and D, respectively.

In the case when there is no significant overlap of the molecular orbitals, so that the interaction energy is dominated by the coulombic interactions, V can be expanded into a power series. In the dipole approximation the interaction is described by:

$$V_{DA} = \frac{1}{4\pi\epsilon_0} \frac{\vec{\mu}_D \vec{\mu}_A - 3(\vec{\mu}_D \hat{R})(\vec{\mu}_A \hat{R})}{R^3} \quad (1)$$

where $\vec{\mu}$ is the electric dipole moment of the molecule D and A, \hat{R} the unit vector between D and A and R the distance between the two molecules. See also [5].

2.1 Energy Transfer

If the interaction is compared in magnitude to the linewidth of the transitions, one can distinguish two limiting cases of the energy transfer. If the interaction energy is larger than the disorder, it is called strong coupling or the exciton picture. In the other limit one talks about weak coupling or incoherent hopping limit. In both cases the transfer rates can be calculated with first order perturbation theory, which leads to Fermi's Golden Rule. For the hopping description, V acts as a perturbation, while in contrast for excitons the coupling between electrons and phonons is the perturbation. In reality the both processes exist. If the real situation can not be described as one of these limits the analysis is challenging.

The disorder has contributions from static (spectral inhomogeneity) and dynamic (electron-phonon interaction) effects. The dynamic contribution can be ruled out by using a low temperature experimental setup, while the static contribution, which is due to small changes in the protein environment, persists.

2.1.1 Weak Coupling

In the limit of weak coupling between A and D the energy transfer rate is described using the Fermi's Golden Rule:

$$k_{D \rightarrow A} = \frac{2\pi}{\hbar} |\langle D^* A | V | D A^* \rangle|^2 \rho(E)$$

where $\rho(E)$ is the density of states of the final manifold of states $|D A^*\rangle$ with the same energy as the initial state $\langle D^* A|$. The total transfer rate is given by the sum over all initial and final states.

The transfer rate is calculated with the dipole approximation for the interaction energy from Eq. (??). As additional assumptions, one has to use that the vibrational relaxation is much faster and that there is no overlap between the electronic wave functions. So for a sufficiently large distance between the molecules the energy transfer rate is:

$$k \propto \frac{\kappa^2 \phi_D}{n^4 R_{DA}^6 \tau_D} \int \varepsilon_A(\nu) f_D(\nu) \nu^{-4} d\nu$$

where ϕ_D is the quantum yield of the donor, ε_A the absorption band of A, f_D the normalized fluorescence of the donor, ν the frequency, n the refractive index of the medium between D and A, R_{DA} the distance between D and A and τ_D the live time of the donor without the acceptor. The integral represent the overlap of the emission spectrum of the donor and the absorption spectrum of the acceptor. The orientation of the dipoles with respect to each other finds its expression in κ in the following manner:

$$\kappa = \cos \alpha - 3 \cos \beta_1 \cos \beta_2$$

Here α is the angle between the dipoles of D and A, β_1 and β_2 the angle of the vector connecting D and A with the transition moment of D and of A, respectively. Distances, where this model is suitable, are in the range of some nm.

In a case where the overlap of the molecular orbitals of D and A can not be neglected, the energy transfer via electron exchange becomes more important. This interaction is referred to as the Dexter mechanism, see [5] for more information.

2.1.2 Strong Coupling

In the case of strong coupling between the molecules, the exciton picture is used. The electronic Hamiltonian

of the complex is given by:

$$H_{el} = \sum_n (E + D_n + \Delta E_n) |n\rangle \langle n| + \sum_{n,m} V_{nm} |n\rangle \langle m| \quad (2)$$

where E is the electronic transition energy of the free monomer, D_n is the shift, caused by dispersive interaction of the n th molecule with its specific environment, leading to spectral heterogeneity, ΔE_n is a random shift, caused by stochastic fluctuations in the environment of the n th molecule. $D_n + \Delta E_n$ is also called the diagonal disorder. V_{nm} describes the dipole-dipole interaction energy between the n th and m th site. Variations over the different V_{nm} of a complex is referred to as off-diagonal disorder, which can be caused by structural disorder or deformation of the arrangement.

The Hamiltonian (2) conserves the number of excitons. The eigenstates separate into classes of linear combinations of site states with a fixed number of molecules excited. Correspondingly, also the eigenvalues of the different manifolds form bands. The separation between consecutive bands is of the order of E , where as the width of the n -exciton band is of the order of $4n \cdot V$. Optical transitions are only allowed between consecutive bands. The random distribution of ΔE_n leads to a localization of the wave function to a limited region of the aggregate. While the Hamiltonian (2) includes only static disorder, also electron-photon interaction can be included into the theory [3, 4], which will cause further localization over time.

The following text will be only concerned with molecular aggregates, which expire strong coupling and can therefore described within the excitonic picture.

2.2 Spectroscopic Properties of Excitons in Aggregates

The molecular exciton approach describes the coherent superposition of the excited states of molecules in aggregates by taking into account their translational symmetry. The spectrum of the complex is calculated by solving the stationary Schrödinger equation. The interactions between the molecules can be treated as perturbations, because of their low strength. The eigenfunctions of the aggregate are then given as linear combinations of the molecular eigenfunctions. In the following paragraphs the interaction of electrons with vibrations is neglected. The complete treatment can be found in [3].

2.2.1 Energy Splitting

With these assumptions the excited state of a dimer can be defined as a linear combination of localized states:

$$\Psi^f = \sum_n c_{fn} \varphi_n^f \prod_{m \neq n} \varphi_m^0 \quad (3)$$

here f enumerates the electronic molecular excitations states, c_{fn} indicates the expansion coefficients and φ_n^f the molecular eigenfunctions. If one takes translational symmetry into account, Ψ^f has to be an eigenfunction of the translation operator $T_{\vec{m}}$, where \vec{m} is an integral number of translational vectors and \vec{k} is the wave vector of the translation operator:

$$T_{\vec{m}} \Psi^f(\vec{k}) = e^{-i\vec{k}\vec{m}} \Psi^f(\vec{k}) \quad (4)$$

If we now assign the molecules in the unit cell the index α , we get from Eq. (4):

$$c_{fn\alpha} = \frac{1}{\sqrt{N}} u_{\alpha\nu}(\vec{k}) e^{i\vec{k}\vec{r}_{n\alpha}} \quad (5)$$

where $u_{\alpha\nu}$ is a unitary matrix for diagonalization, the index ν accounts for degenerate states and N is the number of molecules in the whole aggregate. This can now be applied to the Schrödinger equation and the corresponding characteristic equation will give values for the energy levels of the excitons. Because the matrix, which is describing the resonance interaction is hermitian, all values for the energy levels are real. This results in a splitting into a number of energy levels, which is equal to the number of molecules within the unit cell. The phenomenon is called the Davydov splitting.

2.2.2 Selection Rules and Transition Dipole Strength

The frequency dependent transition dipole moments determine the optical transition spectrum of a molecule. The operator of an aggregate of molecules is represented by the sum of the dipole moment operators:

$$P = \sum_n P_n$$

With Eq. (3) and (5) the exciton transition dipole moment can be calculated to:

$$\langle \Psi_0 | P | \Psi_f(\vec{k}, \nu) \rangle = \frac{1}{\sqrt{N}} \sum_{m,\alpha} u_{\alpha\nu}(\vec{k}) \vec{\mu}_{n\alpha} e^{i\vec{k}\vec{r}_{n\alpha}} \quad (6)$$

In the long wave approximation, the transition dipole moment of the $n\alpha$ th molecule is:

$$\vec{\mu}_{n\alpha} = \langle n\alpha, 0 | P_{n\alpha} | n\alpha, f \rangle$$

For the case of cyclic molecular aggregates $\vec{\mu}_{n\alpha}$ is explicitly dependent on n , and the projection of the optical transition dipole moment on the polarization vector of the external electromagnetic field has to be taken into account. Let us now consider an aggregate with only one molecule per unit cell and an external field with the polarization in parallel with the plane of the aggregate. Without loss of generality we can assume, that one of the molecules is parallel with the polarization of the external field. If the numbering n starts with this molecule, the projection of the dipole moment is given by:

$$\mu_n = \mu \cos \gamma n$$

where $\gamma = 2\pi/N$ is the rotation angle for the n th molecule. Now the projection of Eq. (6) can be written as:

$$\begin{aligned} \mu(k) &= \frac{1}{\sqrt{N}} \sum_n \mu_n e^{ikn} \\ &= \frac{1}{\sqrt{N}} \sum_n \mu \cos(\gamma n) e^{ikn} \\ &= \frac{\mu}{2} (F_+(k) + F_-(k)) \end{aligned}$$

with the definition:

$$F_{\pm}(k) = \frac{1}{\sqrt{N}} \sum_n e^{i(k \pm \gamma)n}$$

the following selection rule is obtained:

$$F_{\pm} = \sqrt{N} \delta_{k, \pm\gamma}$$

The optically allowed state is that, which is next to the lowest exciton state. This result holds not for an external field with the polarization perpendicular to the plane of the aggregate.

A similar calculation for a cyclic molecular aggregate with two molecules per unit cell has shown, that the dipole strength for the transition into the state $k = 0$ vanishes and the transition into states $k = \pm\gamma$ remains [3].

The interaction of the molecules also determines the distribution of the transition dipole strength among the different states. The dipole strength of a transition is given by the sum over the contributions of all

molecules:

$$D_f = \left| \sum_{n=1}^N c_{fn} \vec{\mu}_n \right|^2$$

It can be shown that in the long-wave approximation the sum over all transition dipole strengths is conserved (Thomas-Reiche-Kuhn sum rule):

$$\sum_{f=1}^N D_f = \text{const.}$$

A redistribution can be caused by mixing of states. The mixing occur for example when any kind of disorder, like a random fluctuation or a modulation, is present.

3 The B850 Band of LH2

Rsp. A.'s LH2 is a good model system to check the theory of the previous chapter, because its three dimensional structure is known, there are only three different binding sites and excitons effects are pronounced by the high symmetry.

3.1 Application of Theory

If we apply the specific properties of the B850 complex as outlined in section 1.1 to the Eq. (2), the Hamiltonian will be given through:

$$\begin{aligned} H = & \sum_{n=1}^{18} (E_{0,n} + \Delta E_n) |n\rangle\langle n| \\ & + \sum_{n=1}^{18} (V_{0,n} + \Delta V_n) [|n\rangle\langle n+1| + H.c.] \\ & + \sum_{n=1}^{18} (W_{0,n} + \Delta W_n) [|n\rangle\langle n+2| + H.c.] \end{aligned}$$

where $E_{0,n}$ denotes the site energies of the individual pigments and $V_{0,n}$, $W_{0,n}$ are the nearest- and second-neighbor interactions, respectively. The interaction with the B800 pigments is ignored, which is justified by the distance between them. In a description for low temperatures it is possible to take only the 0-0 transitions into account and to neglect time-dependent exciton localization. It is also assumed that fluorescence occurs only from the lowest energy state in the exciton manifold, because the relaxation process happens at sub

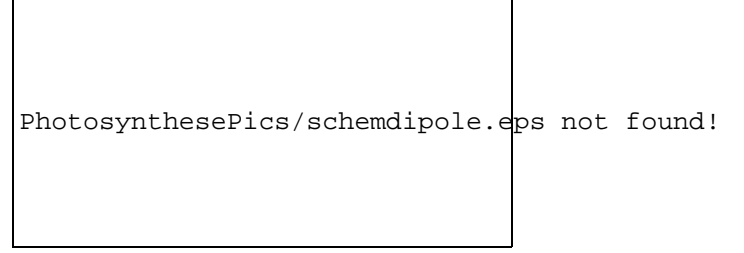


Figure 3: Schematic drawing of the orientation of the transition dipole moments of the individual BChl a molecules and their interactions, Fig. taken from [1]

picosecond timescale. If now the dimer structure of the B850 aggregate is taken into account, see Fig. 3, while disorder is ignored, the energy levels are given by [6]:

$$\begin{aligned} E_k^\pm = & \bar{E} + \bar{W} \cos(k\delta) \\ & \pm \sqrt{E_{EW}^2 + V_i^2 + V_e^2 + 2V_i V_e \cos(k\delta)} \end{aligned} \quad (7)$$

with:

$$\begin{aligned} \bar{E} &= (E_\alpha + E_\beta) / 2 \\ E_{\alpha\beta} &= (E_\alpha - E_\beta) / 2 \\ \bar{W} &= (W_\alpha + W_\beta) \\ W_{\alpha\beta} &= (W_\alpha - W_\beta) \\ E_{EW} &= E_{\alpha\beta} + W_{\alpha\beta} \cos(k\delta) \end{aligned}$$

Because of the the in plane configuration of the pigments in the aggregate the transition dipole moment has a large in plane component, which is concentrated nearly only in the $k = \pm 1$ degenerate pairs, because of the essentially anti-parallel orientation of the dipoles in the dimers. A small out-of-plane component gives rise to a finite oscillator strength of the $k = 0$ level, which is further strengthened by the random diagonal disorder from stochastic variations in the protein environment. Random off-diagonal order originates from irregularities in the orientations and positions of the individual transition dipoles. If for both kinds of disorder the same distribution of perturbations strength is present (e.g. Gaussian), the effects are indistinguishable.

Experimental data suggest that the LH2 aggregate is subject to a modulation, which can be described as a $\cos(2\Theta)$ factor in the first and second order interaction, where Θ corresponds to the angular position in the pig-

ment ring. The Hamiltonian for this configuration is:

$$\begin{aligned}
 H = & \sum_{n=1}^{18} (E_{0,n} + \Delta E_n) |n\rangle\langle n| \\
 & + \sum_{n=1}^{18} (V_{0,n} + V_{mod} \cos [2\phi(n + 1/2)]) \\
 & \cdot [|n\rangle\langle n + 1| + H.c.] \\
 & + \sum_{n=1}^{18} (W_{0,n} + W_{mod} \cos [2\phi(n + 1/2)]) \\
 & \cdot [|n\rangle\langle n + 2| + H.c.]
 \end{aligned}$$

here $\phi = 2\pi/18$. V_{mod} and W_{mod} are the amplitudes of the modulation for the first and second order interaction, respectively.

The $\cos(2\Theta)$ perturbation couples only to exciton states with $\Delta k = \pm 2$. Therefore, the dominant effect of this C_2 perturbation is a coupling between the degenerate $k = \pm 1$ states. Their degeneracy is lifted by a splitting of $2(V_{mod} + W_{mod})$. Effects on other k levels are relatively small. Further more the oscillator strength is redistributed among the exciton states.

3.2 Experimental Setup and Sample Preparation

Hydrolyzed polyvinyl alcohol was purified and added to a buffer containing LH2 complexes from *Rsp. A*. The solution was spin coated on a LiF substrate. The film had a thickness of less than $1 \mu\text{m}$.

The samples were illuminated for the fluorescence microscopy and fluorescence excitation spectroscopy with a tunable CW Ti:Sapphire laser. To obtain the fluorescence spectrum of a single LH2 complex, first a wide-field image was taken with a CCD camera. From this image a well separated complex was selected and the setup was switched to confocal mode, to overcome low read-out rate and low background suppression of the CCD camera. Now the excitation wavelength was scanned and the fluorescence was detected by an avalanche photodiode at 890 nm with bandwidth of 20 nm. To reduce the effect of light-induced fluctuations of the fluorescence intensity on a time-scale of seconds, the spectra were scanned with a speed of 3 nm per second and an integration time of 10 ms per data point. This lead to a spectral resolution which is higher when that of the laser (1 cm^{-1}). For most spectra about 70 scans were added. See for more experimental details [7]. Polarization dependence was examined with a

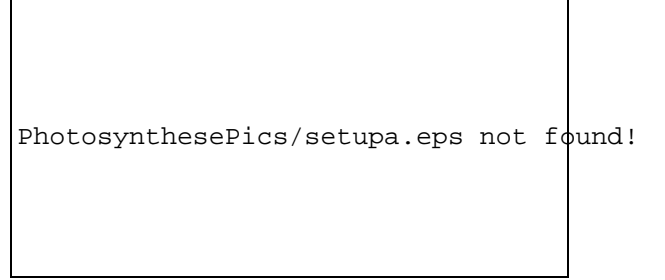


Figure 4: Schematic representation of the experimental arrangement for wide-field experiments, Fig. taken from [7].

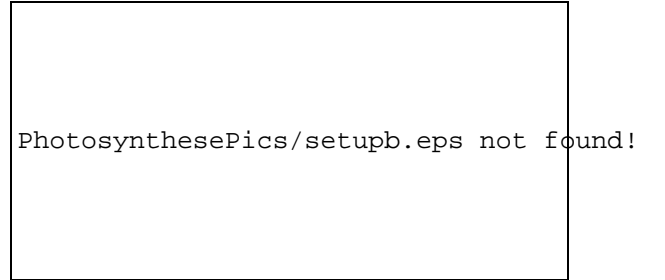


Figure 5: Schematic representation of the experimental arrangement for confocal experiments, Fig. taken from [7].

$\frac{\lambda}{2}$ plate in the confocal light path. With steps of 30° six spectra of each individual complexes were taken.

3.3 Results

In Fig. 6 the upper two spectra show fluorescence-excitation spectra of an ensemble (dashed line) and the sum of spectra of several individual complexes (solid line). These lines match very good. The five lower spectra are recorded from different individual LH2. An inner structure, that was hidden by the ensemble average, becomes visible. Remarkably the B800 band consists out of several sharp peaks. This indicates a strong localization [7]. In the B850 band two broad maxima at around 860 nm are observed, which have mutually orthogonal polarization (Fig. 7). These are assigned to the $k = \pm 1$ exciton states. The splitting of the $k = \pm 1$ states is about 110 cm^{-1} . Using a different matrix (glycerol) showed that the splitting does not originate from the polymer matrix. 40% of the complexes showed a third line at a shorter wavelength, which is attributed to higher exciton states. From the polariza-

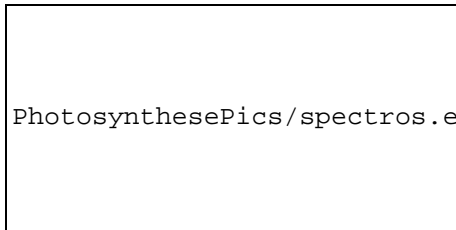


Figure 6: Fluorescence-excitation spectra of LH2 complexes of *Rsp. A.*, the upper traces show the comparison between an ensemble spectrum (dashed line) and the sum over 19 spectra recorded from individual complexes (solid line). For each complex six spectra with different polarizations were summed. The five lower spectra are from single LH2. Fig. taken from [8].

tion dependence it could be further concluded that the LH2 complexes were aligned parallel to the substrate, which might be caused by the spin coating procedure and the low thickness of the film.

A good check for the exciton model is the observation of $k = 0$ transition. From the lifetime of that state (1 ns) a relatively sharp absorption line is expected. To overcome spectral diffusion, the position of the line was determined through a fit of a Lorentzian and the spectra were shifted to line-up all $k = 0$ transitions before ad-

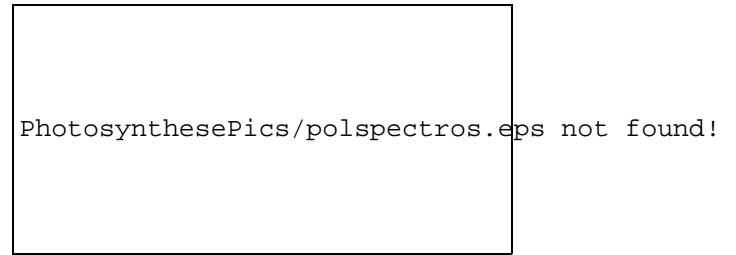


Figure 7: (a) Polarization dependence of the fluorescence-excitation spectra of the B850 spectral region of three individual LH2 complexes. (b) Distribution of the spectral positions for 19 complexes of the three observed bands. Fig. taken from [1].

dition. Note, that through this procedure the rest of the spectra becomes mixed up. It seems that the splitting of the $k = \pm 1$ state is accompanied by a rise in oscillator strength of the $k = 0$ transition. Further conclusions can not be drawn because of the poor statistics.

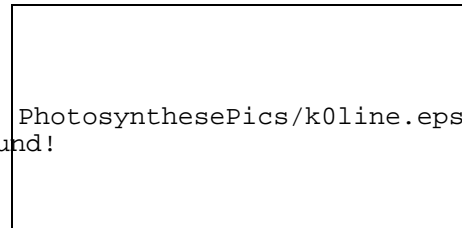


Figure 8: Fluorescence-excitation of the long wavelength part of the B850 spectrum of three different complexes, featuring a sharp peak. The spectra have been aligned for this $k = 0$ transition, before summation, to compensate for spectral diffusion, Fig. taken from [1].

3.4 Discussion

The above mentioned experimental data fully support the theory outlined in section 3.1. Random diagonal disorder will redistribute oscillator strength mainly from the $k = \pm 1$ states to the $k = 0$ and $k = \pm 2$ states. But if one calculates the interaction strength required for the explanation of the 841 nm peak with Eq. (8), the values are far too big with respect to theoretical calculations. Further a large disorder has to be introduced to explain the 110 cm^{-1} splitting of the $k = \pm 1$ states, which is not seen in the broadening of the spectrum.

To explain these experimental data, a C_2 -type modulation is introduced. This deformation will couple states with $\Delta k = \pm 2$ and oscillator strength from the $k = \pm 1$ states is transferred to the $k = \pm 3$ states. If now with a point-dipole approximation the interaction is calculated, the results are in the range which is currently accepted. A splitting of the $k = \pm 3$ state could not be observed because of the signal to noise ratio. The modulation model is further supported by the ratio of the two other peaks in the B850 band. The ratio is expected to be one for pure random disorder, but the experimental data does not contain this value.

A C_2 -type modulation can have different arrangements of the pigments in the complex. Calculations on three models have shown that only the one model fits the experimental data (model C in [6]), in which the inter-pigment-distance on the ellipse is modulated in such a way, that it is the longest at the long axis of the ellipse. The pigments are reoriented to preserve their angle with the local tangent of the ellipse.

To explain the splitting of the $k = \pm 1$ state a deformation of $\delta r/r_0 \simeq 7\%$ is necessary. A ratio of $\delta r/r_0 \simeq 8\%$ will lead to the observed intensity ratio of 0.7 between the 856 nm and 864 nm bands, while still maintaining their mutually orthogonal polarization.

Let us now consider the influence of disorder on the spectra. Fig. 9 shows (a) the distribution of energy splitting, (b) intensity ratios and (c) the angle between the $k = \pm 1$ transitions. This data shows clearly heterogeneity among the B850 pigments, which can be caused by diagonal and off-diagonal disorder. Further more it can be expected that also the elliptical deformation is subject to a distribution. To model these different kind of disorder, first individual complexes with constant amplitude of the deformation were simulated. In a second step the variations of an ensemble were added.

In Fig. 9 a the solid squares represent the results of a Monte Carlo simulation with a deformation amplitude of $\delta r/r_0 \simeq 8.5\%$ and an intracomplex disorder with a FWHM of 250 cm^{-1} . The disorder causes mixing, which leads to a shift of the k states compensating the modulation amplitude slightly. Therefore the amplitude for the model with disorder is higher than for that without disorder. The value of the disorder is an upper limit, because the experimental condition may include other disorder effects. The simulation also predicts a splitting of the $k = \pm 3$ state, but this could not be confirmed by the experiment. First, the disorder given is the upper limit. Second, the signal to noise ratio was not sufficient to fully resolve a small splitting. A disorder value of

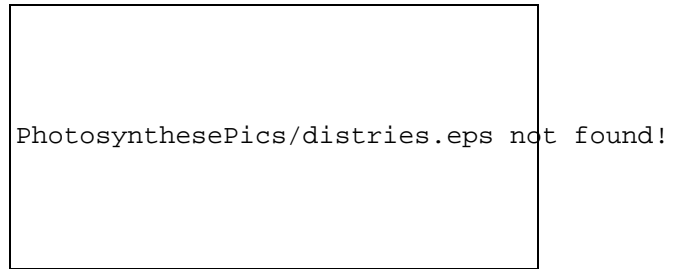


Figure 9: Comparison between histograms from experimental data and numerical simulations (solid squares). (a) Energy separation of the two $k = \pm 1$ transitions, (b) Intensity ratio 864/856 of the two $k = \pm 1$ transitions. (c) Mutual angle between the $k = \pm 1$ transition-dipole moments. (d) The shape of the B850 ring with the orientations of the molecular transition moments, with an elliptical deformation of $\delta r/r_0 = 8.5\%$. Fig. taken from [1].

250 cm^{-1} FWHM alone can not explain the ensemble spectrum, because the splitting of the $k = \pm 1$ states is still visible (Fig. 10, solid line). But the difference in the environment of the individual LH2 complexes have not considered in the simulation until now. From the B850 band this influence can not be determined, because of the strong interaction between the pigments. Therefore, the intercomplex diagonal disorder of the B850 is estimated from the data of the B800 band. Monte Carlo simulations (Fig. 10, dashed line) reproduce now nicely the experimental data (Fig. 10, dotted line). It is important to distinguish between inter- and intracomplex disorder, because only intracomplex disorder will influence the delocalization length of an exciton.

3.5 Conclusion

It was shown that the spectroscopy of individual light-harvesting complexes can provide substantial information for the understanding of photosynthesis. While x-ray crystallography provides structural data of a crystal, spectroscopy allows to investigate the function.

The recorded data allows to verify data from simulations. Through those investigation it was even possible to find an interesting contradiction between crystallographic structural data and spectroscopic data. For the future it would be interesting to investigate parts of the PSU in its natural environment, the membrane.

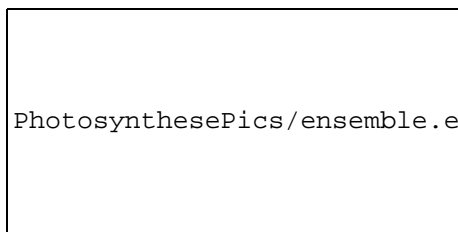


Figure 10: Comparison between the experimental (solid line) and two simulated ensemble spectra of LH2 with $\delta r/r_0 = 8.5\%$. Dashed line: Only intracomplex heterogeneity is taken into account. Dotted line: Intra- and intercomplex heterogeneity are included into the simulation. Fig. taken from [1].

References

- [1] Spectroscopy on the B850 Band of Individual Light-Harvesting 2 Complexes of *Rhodospseudomonas Acidophila* I. Experiments and Monte Carlo Simulations, M. Ketelaars, A. M. van Oijen, M. Matsushita, J. Köhler, J. Schmit, T. J. Aartsma, *Biophys. J.* **80**, 1591 (2001)
- [2] Essential Cell Biology, Alberts, Bray, Johnson, Lewis, Raff, Roberts, Walter, Garland, New York (1998)
- [3] Photosynthetic Excitons, H. van Amerongen, L. Valkunas, R. van Grondelle, World Scientific, Singapore (2000)
- [4] Photosynthetic Light-Harvesting: Reconciling Dynamics and Structure of Purple Bacterial LH2 Reveals Function of Photosynthetic Unit, V. Sundström, T. Pullerits, R. van Grondelle, *J. Phys. Chem. B* **103**, 2327 (1999)
- [5] Excited-state dynamics and interactions in pigment protein complexes from photosynthetic bacteria, Simone I. E. Vulto, PhD Thesis, Universiteit te Leiden (1999)
- [6] Spectroscopy on the B850 Band of Individual Light-Harvesting 2 Complexes of *Rhodospseudomonas Acidophila* II. Exciton States of an Elliptically Deformed Ring Aggregate, M. Matsushita, M. Ketelaars, A. M. van Oijen, J. Köhler, T. J. Aartsma, J. Schmit, *Biophys. J.* **80**, 1604 (2001)
- [7] Spectroscopy of individual LH2 complexes of *Rhodospseudomonas Acidophila*: localized excitons in the B800 band, A. M. van Oijen, M. Ketelaars, J. Köhler, T. J. Aartsma, J. Schmidt, *Chemical Physics* **247**, 53 (1999)
- [8] Unraveling the Electronic Structure of Individual Photosynthetic Pigment-Protein Complexes, A. M. van Oijen, M. Ketelaars, J. Köhler, T. J. Aartsma, J. Schmidt, *Science* **285**, 400 (1999)